



Modified chitosan for the collection of reactive blue 4, arsenic and mercury from aqueous media

V. Dhanapal^a, K. Subramanian^{b,*}

^a Department of Physical Sciences, Bannari Amman Institute of Technology, Erode Dt, Sathyamangalam 638 401, Tamil Nadu, India

^b Department of Biotechnology, Bannari Amman Institute of Technology, Erode Dt, Sathyamangalam 638 401, Tamil Nadu, India



ARTICLE INFO

Article history:

Received 7 July 2014

Received in revised form 9 September 2014

Accepted 11 September 2014

Available online 23 September 2014

Keywords:

Dyes

Toxic metals

Remediation

NMR

Adsorption thermodynamics

ABSTRACT

In the present investigation a series of modified chitosan as adsorbents were synthesized free radically at 70 °C using acryloylated chitosan (AC-chitosan) as macromer, 2-acrylamido-2-methyl-1-propansulfonic acid (AMPS), 2-(diethylamino) ethylmethacrylate (DAEMA) as co-monomers and *N,N'*-methylene bisacrylamide (N-MBA) as crosslinker for using as adsorbents in effluent remediation. Their structures (¹H and ¹³C NMR), thermal stability (TG/DTG), surface morphology (SEM), reactive blue 4 (RB4), toxic metals such as arsenic (AsO²⁻) and mercury (Hg²⁺) uptake, swellability and reusability were evaluated. The adsorption of RB4 (701 mg/g), and the uptake of AsO²⁻ (551 mg/g) and Hg²⁺ (455 mg/g) showed Langmuir isotherm behavior with pseudo-first-order kinetics. The diffusion of water, RB4, AsO²⁻ and Hg²⁺ into the matrix followed non-Fickian mechanism. The evaluated changes in Gibbs free energy (ΔG°), entropy (ΔS°) and enthalpy (ΔH°) for adsorption indicated that the process was exothermic.

© 2014 Elsevier Ltd. All rights reserved.

1. Introduction

Increased industrialization and urbanization globally have resulted in the enormous discharge of industrial effluents with colored pigments such as dyes from textile industries and toxic heavy metal ions such as arsenic (As³⁺) from electronic, wood and leather tanning industries (Nami Kartal & Imamura, 2005), mercury (Hg²⁺) from electro chemical, metal extraction and refining industries, etc. seriously polluting soil and water bodies. The typical concentration range of As³⁺ and Hg²⁺ metal ions reported for industrial effluents were 0.25 to 100 mg/L and 0.1 to 100 mg/L, respectively (Dinesh & Pittman, 2007; Anoop Krishnan & Anirudhan, 2002). Such toxic metal ions and dyes beyond certain concentration limits in effluents can cause potential hazards such as skin, lung and kidney cancers and affect digestive system (Rajeswari, Namasisvayam, & Kadirvelu, 2001) of mankind and harmful to other living beings if improperly handled. A very high exposure to inorganic arsenic can cause infertility, skin disturbances, declined resistance to infections, heart disruption, and DNA and brain damage (Musico, Santos, Dalida, & Rodrigues, 2013). Inorganic mercury poisoning is associated with psychological changes, spontaneous abortion and congenital

malformation. In addition, the organic monomethylmercury causes damage to the brain and the central nervous system and reduction in root growth of aquatic plants. The unabsorbed dyes from the textile dying effluents are having low biochemical oxygen demand and high chemical oxygen demand values (Rajeswari et al., 2001). Besides, they are threatening the aquatic life, agricultural cultivation and underground water even at trace levels. Hence it is necessary to remove these toxic metal ions and dyes from the effluent to the tolerable level before being discharged into land and water using appropriate methods. Adsorption technique is the widely used cost effective method in the effluent treatment. Generally activated carbon, natural clays (Tahir & Rauf, 2006), modified clays (Baskaralingam, Pulikesi, Ramamurthi, & Sivanesan, 2006), fly ash (Dhadapkar, Rao, Pande, & Kaul, 2006) etc. are considered to be cost effective adsorbents to bring down the concentration of unabsorbed dyes and toxic metal ions from effluents.

In recent years hydrogels are increasingly being used as adsorbents to remove dyes, toxic metal ions and other pollutants from effluent (Paulino et al., 2006; Wang & Liu, 2013) which involves physico-chemical interaction of dyes and chelation of toxic metal ions. Hydrogels, a class of physico-chemically crosslinked three-dimensional network hydrophilic polymers can imbibe and retain considerable amount of water and water soluble substances without dissolving and losing their structural integrity. Due to these properties, they are finding widespread applications (Guilherme et al., 2005) in bioengineering, biomedicine, agriculture, food

* Corresponding author. Tel.: +91 4295 226254/+91 9894372411; fax: +91 4295 226666.

E-mail address: drksubramanian@rediffmail.com (K. Subramanian).

industry, water purification, separation process, effluent treatment etc. It has been reported (Bayramoglu, Yakup Arica, & Bektas, 2007) that the adsorption capacity of hydrogel can be improved by introducing some natural preformed polymer such as alginates (Dhanapal & Subramanian, 2014), chitosan, etc. during hydrogel synthesis or by growing hydrophilic moiety on chitosan/alginate by graft copolymerization of appropriate hydrophilic monomers. Among the polysaccharides, chitosan, chitosan derivatives or chitosan modified by methods such as radical grafting of monomers, reinforcing with clay, blending with other polymers, IPN formation, etc. were widely used as adsorbent materials for the removal of dyes and toxic metal ions from effluents through adsorption or chelation mechanism (Liu, Wang, Yu, & Meng, 2013; Wan Ngah, Teong, & Hanafiah, 2011; Crini & Badot, 2008; Bayramoglu et al., 2007). Chelation is the prevalent mechanism of collection of transition and post-transition metal ions by chitosan amino groups (Muzzarelli & Rocchetti, 1974; Muzzarelli, 1977; Muzzarelli, 2011). Incorporation of highly hydrophilic hydrogel segments on chitosan may improve the collection of metal ions and dyes from aqueous medium through adsorption (Paulino et al., 2006; Wang & Liu 2013). Hence, the present investigation involves linking of hydrophilic segments by copolymerizing the monomers AMPS and DAEMA in presence of a crosslinker N-MBA via the *N*-acryloyl group of chitosan by appropriate synthetic strategy to enhance the adsorption or chelation capacity of modified chitosan.

2. Experimental

2.1. Materials

AMPS, N-MBA (Aldrich) were purchased and used as received. DAEMA (Aldrich) and acrylic acid (AA, Himedia, Mumbai) were purified by column chromatography. Potassium persulphate (KPS, NICE, Cochin) and chitosan were used after recrystallization in distilled water and re-precipitation, respectively. Hydrochloric acid (HCl), potassium iodide (KI), RB4, rhodamine-B (RhB) (Himedia, Mumbai), benzoyl chloride (BC), hydroquinone (HQ), *N,N'*-dimethyl formamide (DMF), dimethyl sulfoxide (DMSO), poly(vinyl alcohol) (PVA), mercury(II) chloride, sodium arsenite (Merck), acetone, methanol, sodium hydroxide (NaOH), acetic acid (Rankem, New Delhi) were of analytical grade and used as received.

2.2. Synthesis of acryloyl chloride (ACOCl)

ACOCl was synthesized by refluxing AA (0.8 mol), BC (2.66 mol) and HQ (2 g, polymerization inhibitor) in a 500 mL round bottom flask at 80°C for 2 h in nitrogen atmosphere and collecting the fraction distilled at 90°C (Siva Bharathi, Mohan Reddy, Ramachandra Reddy, & Venkata Naidu, 2010). The liberated HCl was trapped in 0.1 N NaOH solution. The collected impure ACOCl was redistilled at 72°C and the fraction (yield 65%) collected was used in subsequent experiment.

2.3. Synthesis of AC-chitosan

A chitosan solution prepared by dissolving ten grams of purified chitosan powder in 50 mL of 1% acetic acid solution taken in a 250 mL round bottom flask was charged with 75 mL DMSO and the mixture was heated to 100°C to facilitate complete dissolution of chitosan. To this 20 mL of DMF and 1.5 mL of pyridine were added under continuous stirring over a period of 5 min and then cooled to 0°C. In sequence, 3 mL of ACOCl in 5 mL DMF were drop wise added to this solution with constant stirring and left aside for 2 h at 0°C (Jayakumar, Prabaharan, Reis, & Mano, 2005; Pourjavadi, Jahromi, Seidi, & Salimi, 2010). The AC-chitosan thus formed was

precipitated in acetone and repeatedly washed with acetone, air dried and stored for further use.

2.4. Synthesis of ACAD

Twenty two samples of ACADs as adsorbent materials with different compositions designated by ACAD-0, ACAD-1, ACAD-2... ACAD-20 and ACAD-21 were synthesized by radical copolymerization by taking various amounts of AC-chitosan, AMPS and DAEMA using N-MBA as a crosslinker and KPS as thermal initiator in a 50 mL stoppered borosilicate tube, at 70°C after nitrogen purging. Thus obtained ACADs were recovered by adding ice cold methanol and washed repeatedly with methanol. Then the crosslinked gels were cut into small pieces and dried to constant weight at 50°C in an air oven. Further, these ACADs were powdered and purified by Soxhlet extraction using acetone-methanol (1:1 v/v), at 70°C for 48 h. The purified ACADs were powdered, sieved and stored after vacuum drying.

2.5. Characterization techniques

The NMR spectra were recorded on Bruker Avance III 500 MHz multi nuclei NMR spectrometer at 500 MHz for ¹H and 125 MHz for ¹³C (proton decoupled) in CD₃COOD/D₂O mixed solvents taking solvent peak as reference. TG/DTG studies were performed on TGA Q 500 V20.10 Build 36 with a sample size of 1.5–3.5 mg under air at a heating rate of 10 °C/min for the temperatures range from ambient to 800°C. The concentrations of dye and those of AsO²⁻ and Hg²⁺ metal ions were estimated spectrophotometrically on Perkin Elmer Lambda 35 UV-vis absorption spectrometer at 575 nm for dye and at 554 and 592 nm for metal ions complex with Rh B. SEM micrographs of equilibrium swelled, lyophilized ACAD and AsO²⁻ adsorbed ACAD at different magnifications were recorded on ZEISS EVO series SEM model EVO 50 microscope.

2.6. Water uptake measurements

The degree of water uptake of ACADs were measured using tea bag method (Dhanapal, Vijayakumar, & Subramanian, 2013) by taking 0.1 g of sieved ACAD sample in 200 mL of deionized water at 30°C under equilibrium swelling conditions (6 h). The swelling profiles ACADs were constructed by plotting the water uptake vs. time at 30°C. An average of three measurements were taken to calculate equilibrium swelling (ES) using the following equation:

$$ES = \frac{W_s - W_d}{W_d} \quad (1)$$

where W_s and W_d are the weights of the swollen and the dry polymer samples, respectively.

2.7. Column mode adsorption of metal ions and dye

Separate stock solutions of AsO²⁻ and Hg²⁺ were prepared by dissolving 1.733 and 1.350 g of sodium arsenite and mercury(II) chloride, respectively in 1000 mL deionized water. A series of RB4 solution of different concentrations (1, 2, 3, 4 and 5 × 10³ mg/L) were prepared. The adsorption studies of AsO²⁻, Hg²⁺ and dye from their respective solutions were performed on all ACAD samples at different swelling time, temperature and pH. The adsorption experiments were done using separate identical glass columns of 2 cm diameter and 86 cm length. The columns were filled with 10 g of powdered and sieved adsorbents (ACADs) without voids. Then, the synthetic effluent prepared using metal ion/or dye were eluted through these columns at a constant flow rate (2 mL/min) at 30°C. The effluent solutions were collected at different time intervals and the concentration of metal ions and dye in the collected

fractions were estimated spectrophotometrically. An average of triplicate was taken for metal ions and dye concentrations. Similarly the adsorption capacity of virgin chitosan was tested for these adsorbates. The simultaneous removal (Tastan, Ertugrul, & Donmez, 2010) of dye and metal ions was also tested using a synthetic composite effluent containing RB4 (5.3×10^{-4} mol), AsO_2^- (1.1×10^{-3} mol) and Hg^{2+} (1.23×10^{-3} mol). Besides, the adsorption capacity of ACADs (showed maximum uptake behavior) were also compared to the reported (Bayramoglu et al., 2007; Pourjavadi et al., 2010) values on other adsorbents and virgin chitosan. The amount of dye and metal ions uptake were calculated as per the mass balance in the following equation:

$$q_e = (C_i - C_e) \frac{v}{w} \text{ mg/g} \quad (2)$$

where q_e , C_i , v and w are the equilibrium amount of metal ion/dye adsorbed onto the adsorbents (mg/g), the initial concentration of metal ion/dye in the dye effluent (mg/L), the equilibrium concentration of the metal ion/dye in solution (mg/L), the volume of the metal ion/dye solution (L) and the weight of the adsorbent (g), respectively.

2.8. Estimation of adsorbed metal ions and RB4 dye in treated effluent

To estimate the amount of AsO_2^- ions, 20 mL of eluate containing residual AsO_2^- ion was taken in 50 mL standard flask. To this 4 mL each of KI solution and con. HCl were added and then the mixture was shaken gently, followed by the addition of 8 mL of 0.05% RhB. Then this was made up-to 50 mL with distilled water and then left aside for 15 min and then its absorbance was measured at 554 nm. For the estimation of Hg^{2+} , 2 mL each of 10.8 M H_2SO_4 and 0.15 M KI solution were added to 20 mL of eluate containing residual Hg^{2+} was taken in a 50 mL standard flask and shaken for a min. Subsequently 2 mL of RhB (5×10^{-4} M) and 5 mL of 1% PVA were added to the above solution and made up-to 50 mL, and left aside for 10 min and the absorbance of complex formed was measured at 592 nm (Ajai, Sunita, & Gupta, 2000; Yow loo et al., 2012). The amount of metal ions, dye uptake and its molar absorption coefficient values were calculated using Beer–Lambert law equation (Ajai et al., 2000; Yow loo et al., 2012).

2.9. Adsorption isotherm modeling

In any adsorption experiment the equilibrium adsorption isotherm data can explain the interactive behavior between adsorbate and adsorbents, and the isotherm data will be useful for the selection of an adsorbent for a particular adsorbate. The equilibrium relationship between an adsorbate and adsorbent was correlated by several expressions (Dhanapal & Subramanian, 2014) which are used to describe isotherm modeling. In the present investigation the isotherm data were fitted for the Langmuir and Freundlich models as per Eqs. (3) and (4), respectively, since majority of adsorbent–adsorbate systems obeyed these two models.

$$\frac{1}{q_e} = \frac{1}{q_m} + \frac{1}{q_m K_L C_e} \quad (3)$$

$$\log q_e = \log K_F + N \log C_e \quad (4)$$

where q_m is the equilibrium monolayer adsorption capacity (mg/g) and the K_L (L/mg, Langmuir constant) value is essentially equilibrium constant. The variation of K_L with temperature can be used to estimate the enthalpy change accompanying adsorption and the affinity between the adsorbent and adsorbate. K_F is Freundlich constant, which predicts the quantity of dye adsorbed (mg/g) per g of polymer under equilibrium. The values of N indicate the degree of non-linearity between solution concentration and adsorption

2.10. Adsorption kinetics

The metal ions and RB4 adsorption kinetics will be influenced by adsorption reactions, and the mass transfer steps that govern the transfer of metal ions/dye from the respective effluents to the adsorption sites. Hence the kinetics of AsO_2^- , Hg^{2+} and RB4 adsorptions were tested using pseudo-first and second order kinetic models based on Eqs. (5) and (6), respectively.

$$\log (q_e - q_t) = \log q_e - \left(\frac{k_1}{2.303} \right) t \quad (5)$$

$$\frac{dq_t}{dt} = k_2 (q_e - q_t)^2 \quad (6)$$

where q_e and q_t (mg/g) are amounts of AsO_2^- /or Hg^{2+} /or RB4 adsorbed at equilibrium and at time 't', respectively, k_1 (min^{-1}) and k_2 (g/mg/min) are the rate constants for pseudo-first and second order kinetics, respectively.

2.11. Thermodynamics of adsorption

The practical applicability and spontaneity of the adsorption process was evaluated by measuring the changes in thermodynamic parameters such as ΔG° , ΔH° and ΔS° , since they are the actual indicators of adsorption process. The values of ΔG° , ΔH° and ΔS° for AsO_2^- , Hg^{2+} and RB4 adsorptions were determined graphically using the following equation:

$$\ln K_d = \frac{\Delta S^\circ}{R} - \frac{\Delta H^\circ}{RT} \quad (7)$$

where K_d is the distribution coefficient of the adsorbate ($K_d = q_e/C_e$), which is a measure of adsorption capacity of ACAD, R is the universal gas constant (8.314 J/K/mol) and T is the absolute temperature (K). The plot of $\ln K_d$ vs. $1/T$ yields a straight line with $-\Delta H^\circ/R$ and $\Delta S^\circ/R$ as slope and intercept, respectively.

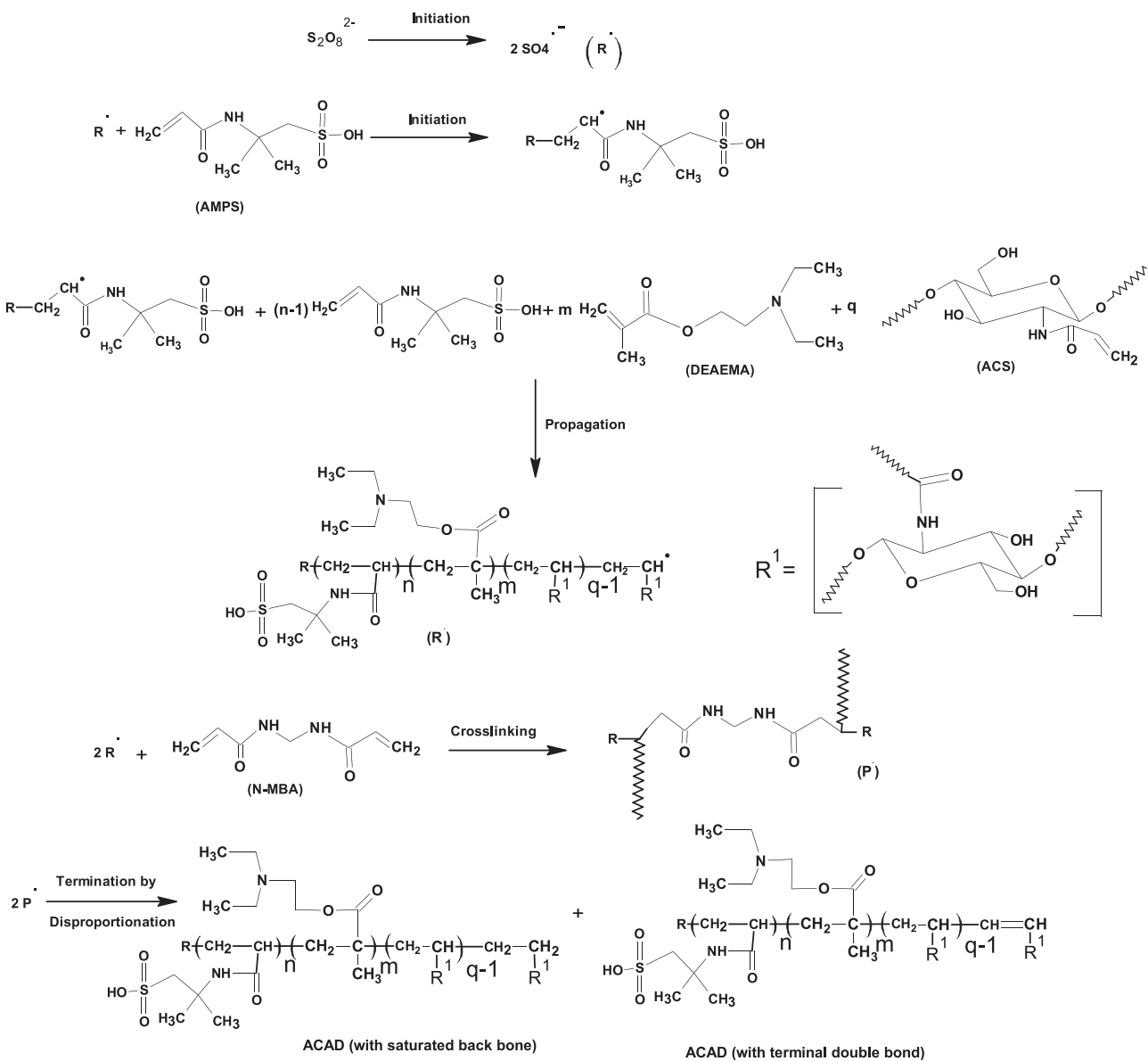
3. Result and discussion

3.1. Mechanism of polymerization

The mechanism for the formation of ACAD by free radical graft copolymerization is shown in Scheme 1. The termination of growing polymer radical may occur either by coupling or disproportionation route or by chain transfer mechanism involving monomer, polymer or by primary radical (Dhanapal & Subramanian, 2014). If termination occurs through disproportionation terminal double bonds may be introduced in the dead polymer, unlike the termination by coupling which will produce saturated polymer.

3.2. ^1H and ^{13}C NMR analysis

The representative ^1H and ^{13}C NMR spectra of chitosan and AC-chitosan are displayed in Fig. 1. The ^1H NMR spectrum of chitosan (Fig. 1(a)) showed a signal at 4.7 ppm corresponding to the $\text{C}_1\text{—H}$ proton of the glucosamine ring, while the signals between 3.05 and 4.20 ppm correspond to the hydrogen atoms bonded to C_2 , C_3 , C_4 , C_5 and C_6 carbons of the glucosamine unit. The observed ^1H NMR signals (Fig. 1(b)) in the range 5.93–6.95 ppm for AC-chitosan are attributed to the olefinic and amide protons in $-\text{NH}\text{—CO}\text{—CH=CH}_2$ group, which indicate the presence of acryloylated amino group in the glucosamine ring (Pourjavadi et al., 2010). These signals were absent in the ^1H NMR of chitosan (Fig. 1(a)). The signals at 11.5, 2.2 and 4.78 ppm are due to solvent peaks of residual protons in the deuterated solvents. Similarly the resonance signal at 97.2 ppm in the ^{13}C NMR spectra of chitosan (Fig. 1(c)) and AC-chitosan (Fig. 1(d)) is assigned to C_1 atom of chitosan and AC-chitosan. The

**Scheme 1.** Mechanism for formation of ACAD.

resonance signals in the region 55–79 ppm correspond to $\text{C}_2\text{--}\text{C}_6$ atoms of chitosan and AC-chitosan. The signals at 179.2, 129.6 and 138.7 ppm are attributed to the carbons of $>\text{C=O}$, $=\text{CH}_2$ and $-\text{CH}=$ of acryloylamido group, respectively and those at 19.2 and 177.2 ppm are due to solvent. The average degree of substitution (DS, acryloylation) was calculated from the integrals of the ^1H NMR signals of acryloyl and $\text{C}_1\text{--H}$ protons using the following equation:

$$\text{DS} = \frac{(\text{Integral of protons of } -\text{CO}-\text{CH}=\text{CH}_2)/3}{\text{Integral of proton } \text{C}_1} \quad (8)$$

and the value of DS was found to be 0.282.

3.3. Thermogravimetric (TG) analysis

The representative TG thermograms of ACAD samples shown in Fig. 2(a) indicated multistep degradations. The initial weight loss up to 100°C was attributed to loss of moisture and other volatile impurities present in ACAD. The degradations of ACAD-0 (prepared without AC-chitosan) and ACAD-13 around 245–250°C was

assigned to decomposition via the sulfonate and amide groups, olefinic bonds, etc. (Diao, Yan, Qiu, Lu, Lu & Lin, 2010; Zhu et al., 2012). The weight loss around 345–350°C was more likely due to the degradation initiated via decarboxylation of carboxylate anion, scission of crosslinks (Dhanapal et al., 2013) etc. The weight loss at 395 and 405°C were due to the degradations of methacrylate moiety and of the stabilized product formed during earlier stage of thermal degradations (Diao et al., 2010) in ACAD-0 and ACAD-13. The degradation of ACAD-13 around 480°C was more likely due to a complex process involving dehydration of gulcosamine rings, decomposition of acetylated and deacetylated units of chitosan (Zhu et al., 2012). These thermal features of ACAD-13 in air indicated that the modified chitosan was thermally stable enough to withstand the adverse environmental conditions in air for continuous and prolonged applications.

3.4. Water, metal ions uptake and dye adsorption

The water, metal ions and dye uptake studies for all ACAD samples revealed that the sample ACAD-13 had adsorbed higher

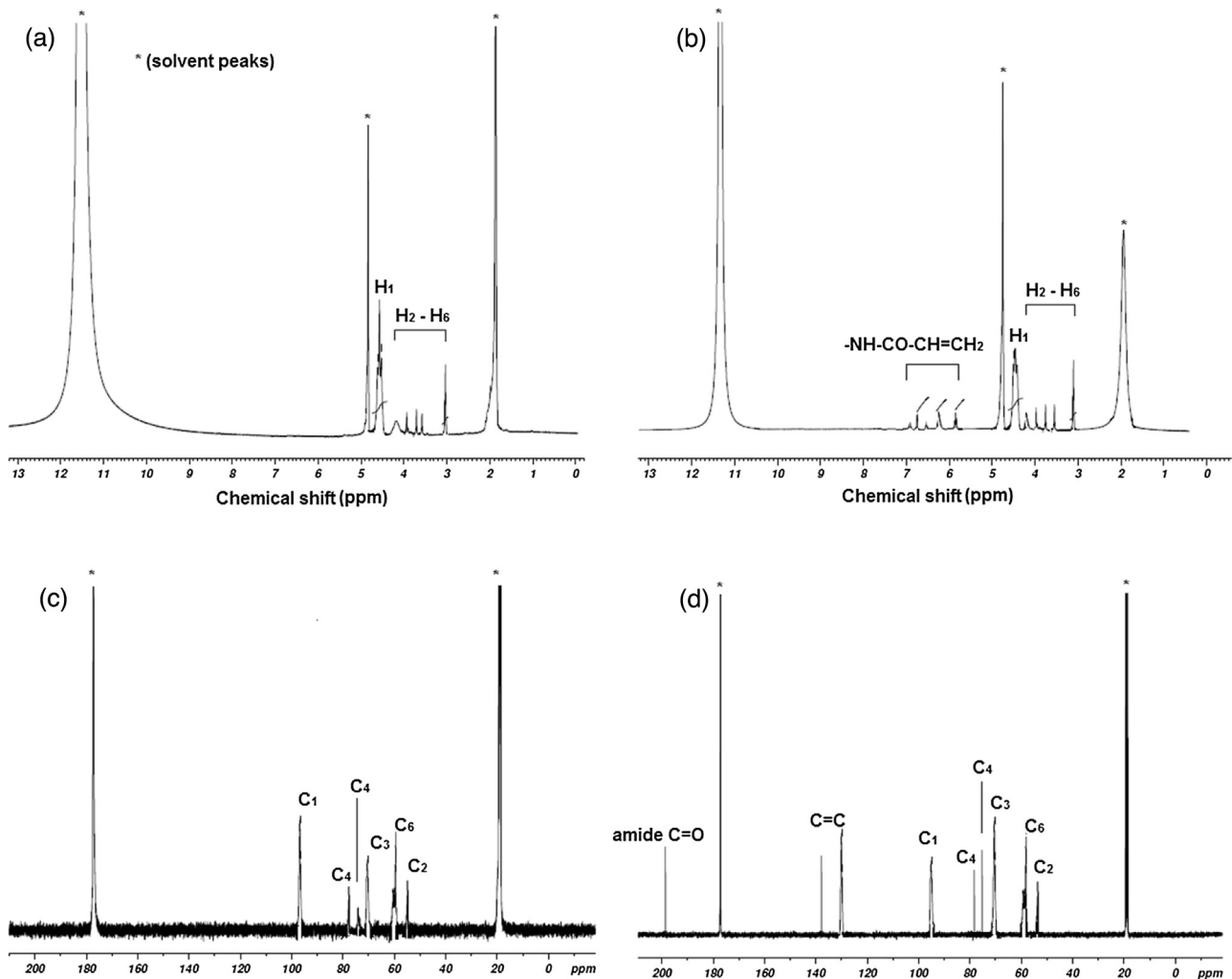


Fig. 1. Representative ¹H (Chitosan, (a)) and AC-chitosan (b)) and ¹³C (chitosan (c), AC-chitosan (d)) NMR spectra.

amounts of Hg²⁺(455 mg/g) AsO²⁻ (551 mg/g) and RB4 (701 mg/g) at 30°C compared to those observed for other samples. Hence, the extent of metal ions, dye and water uptake profiles with respect to time were given only for ACAD-13 and chitosan (Fig. 2(b)). These values for virgin chitosan were 223, 257 and 323 mg/g, respectively for identical experimental conditions. The significant difference in the adsorption capacities of virgin and modified chitosan was more likely due to its increased swellability and three dimensional network structures due to hydrophilic segments and crosslinking, respectively. During the simultaneous removal of toxic metal ions and RB4, the RB4 adsorption was not affected by toxic metal ions even though the effluent contained considerable amount of Hg²⁺ and AsO²⁻ metal ions. Here only 233 and 275 mg/g of Hg²⁺ and AsO²⁻, respectively were chelated/adsorbed and these values were much less than those observed when they were present separately. This may be attributed to a competition for the metal ions to get chelated and dye molecules to get adsorbed at the reactive sites of adsorbent. Hence the chelation of AsO²⁻ and Hg²⁺ were significantly altered due to the extent of metal ion-ligand interaction and competition between dye and metal ions for the active sites of adsorbent. It is worth noting that the adsorption capacity of ACAD-13 was significantly higher than the reported values for other materials (Bayramoglu et al., 2007; Pourjavadi et al., 2010; Liu et al., 2013; Wan Ngah et al., 2011;) and virgin chitosan. Crini et al., 2008

3.5. SEM

The surface morphological features of equilibrium swelled lyophilized ACAD-13, ACAD-21, metal ion adsorbed ACAD-13 were probed using SEM and the typical representative SEM micrographs are given in Fig. 3. Analysis of these micrographs implied the formation of pores and porous network structures during freeze drying of synthesized ACAD. These were attributed to water loss by evaporation and crosslinks in ACAD-13. The distribution of pores massively in the freeze dried samples (Figs. 3(b and d)) indicated uptake of water and AsO²⁻ throughout the bulk of the material and presence of void volume. The average diameter of the pores calculated by assuming spherical shape for these pores was found to be 6 μm . The uneven pores sizes (Fig. 3(b)) may be due to the heterogeneity in the adsorbent. These pores may be the areas, where water, metal ions permeate and form secondary bond with dyes and metal ions (Pourjavadi & Barzegar, 2009). The influence of crosslinker on the surface morphological features of the adsorbent was explained using the SEM micrograph of ACAD-21 (prepared without crosslinker) and it is given in Fig. 3(c). In the absence of crosslinker few pores were observed on the surface of ACAD-21, and less extent of water and metal ions uptake for ACAD-21 were also corroborated by the lack of pores structure and void volume. Analysis of Fig. 3(d) implied the adsorption/chelation of AsO²⁻ on ACAD-13 which can be well supported by the presence of highly heterogeneous pores

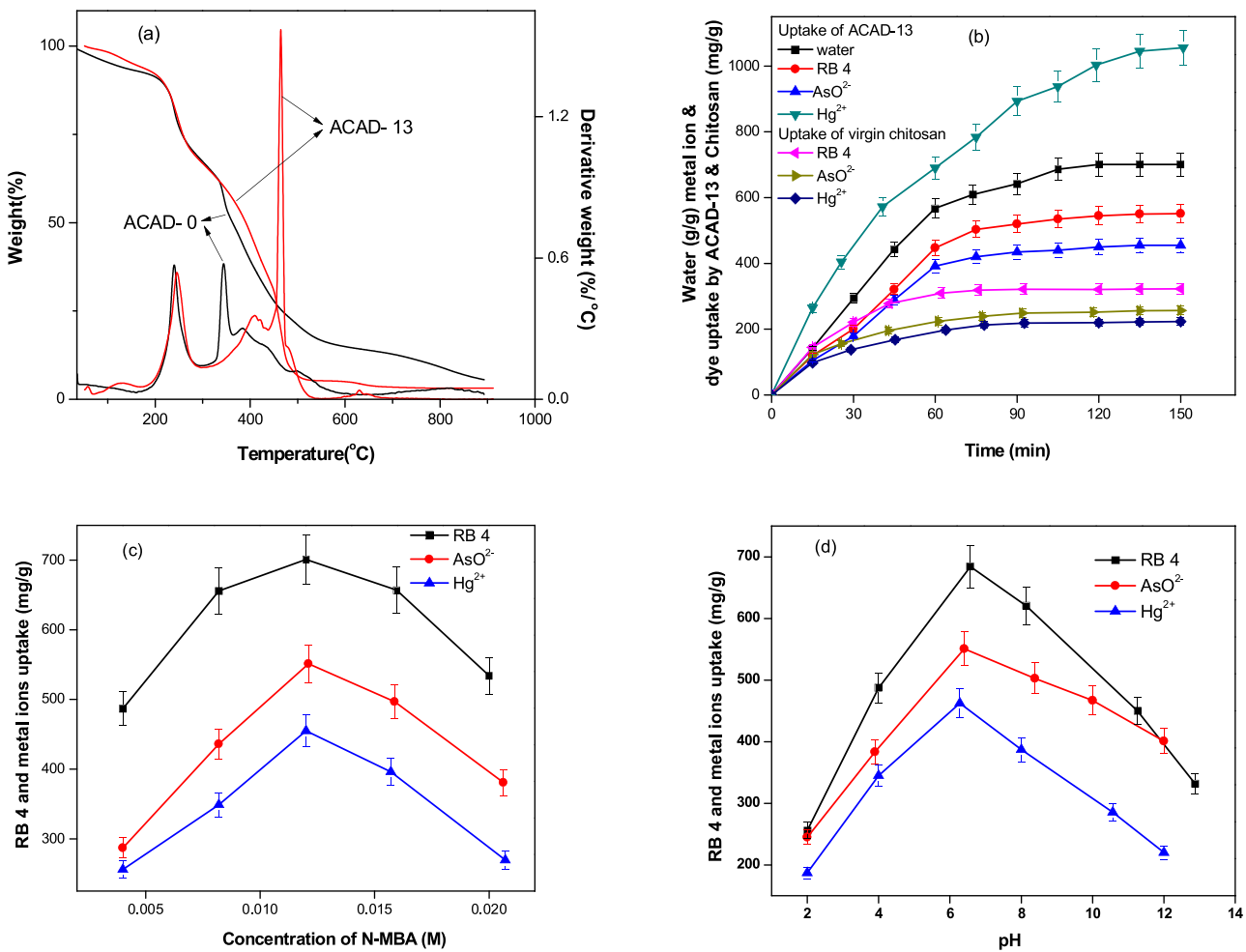


Fig. 2. TG/DTG traces (a) of ACAD-0 and ACAD-13, (b) water, RB4, AsO²⁻ and Hg²⁺ uptake profiles for ACAD-13 and virgin chitosan, effect of (c) N-MBA and pH (d) on dye and toxic metal ions uptake of ACAD-13.

within the sample before adsorption (Fig. 3(b)) while the pores were observed to be packed with metal ion after adsorption. The porous structure appeared to be the predominant cause for the high swellability, and dye and metal ions uptake.

3.6. Adsorption isotherms

The adsorption data for Hg²⁺ and AsO²⁻ metal ions and RB4 dye on ACAD-13 were tested for Langmuir, and Freundlich isotherms models by curve fitting as shown in Fig. 4. The correlation coefficient of (R^2) Langmuir isotherm (Fig. 4(a)) for these adsorbates indicated mono layer uptake. This was also supported by the nearly identical adsorption values for these adsorbates measured experimentally and calculated theoretically under equilibrium conditions on ACAD-13 for Langmuir adsorption. Hence, it appears that the Langmuir model described well the uptake of metal ion and RB4 on ACAD-13 and the calculated isotherm parameters q_m and K_L from the slope and intercept of the Langmuir plot $1/q_e$ vs. $1/C_e$ (Fig. 4(a)) are given in Table 1. The K_L and q_m values for organic dye seems to be more due to more interaction of organic dye with organic matrix than the metal ions (inorganic) interaction with organic matrix.

3.7. Adsorption kinetics

The degree of metal ions and dye uptake were tested with the pseudo-first and second order kinetic models and the better model

was identified by comparing the R^2 (Table 2) values of the plot $\log(q_e - q_t)$ vs. t' and t/q_t vs. t , respectively (Fig. 4(b-d)). This analysis implied that the dye and metal ion uptake followed pseudo first-order kinetics. The rate constants of adsorption determined from the slopes of profiles in Fig. 4(b-d) decreased with temperature, indicating that enhanced temperature does not favor the adsorption of RB4/metal ions which may be attributed to the decrease in activation energy.

3.8. Thermodynamics of adsorption

The effect of temperature on the adsorption process can be understood by analyzing the change in thermodynamic parameters such as ΔG° , ΔH° and ΔS° for metal ions and dye as per Eq. (9) and their values are given in Table 3. The negative values of ΔG° for the temperatures 303, 313 and 323 K indicated that the metal ions and RB4 adsorption on ACAD-13 were spontaneous. The average negative ΔH° value for the above temperatures indicated adsorption was exothermic which may be due to the weak interactions such as hydrogen bonding, salt-like interaction, etc. between the adsorbent and adsorbate. The positive ΔS° value for the adsorption may be attributed to the increased randomness at the solid-solution interface (Dhanapal & Subramanian, 2014) due to the increased segmental mobility of the swollen polymer and release of hydrated water molecules from the dye and metal ions.

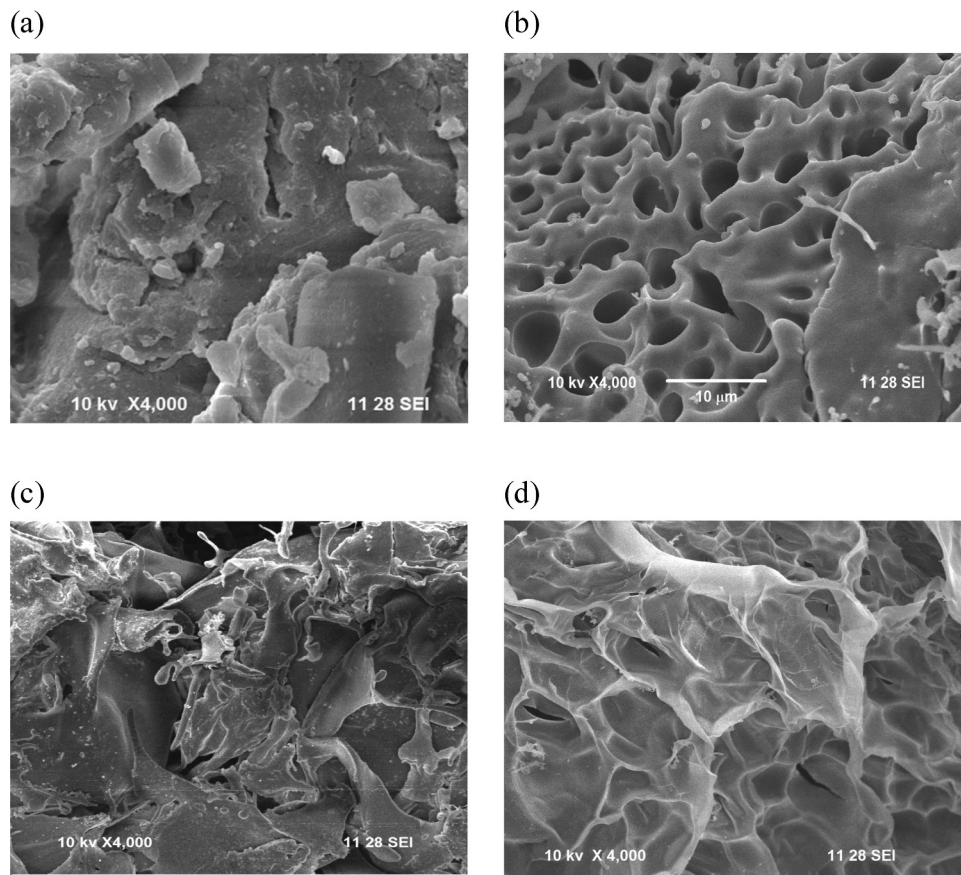


Fig. 3. SEM micrographs of as synthesized ACAD-13 (a), freeze dried ACAD-13 (b), ACAD-21(c) and AsO²⁻ adsorbed ACAD-13 (d).

Table 1

Langmuir and Freundlich adsorption isotherm parameters for ACAD-13/RB4, ACAD-13/AsO²⁻ and ACAD-13/Hg²⁺ systems.

Adsorbent code	Adsorbate	Langmuir isotherm parameters		
		q_m (mg/g)	K_L (L/mg)	R^2
ACAD-13*	RB4	676	4.127	0.986
	AsO ²⁻	494	2.869	0.987
	Hg ²⁺	421	1.843	0.981
Adsorbent code	Adsorbate	Freundlich isotherm parameters		
		K_F (mg/g)	N	R^2
ACAD-13*	RB4	4.81	0.405	0.931
	AsO ²⁻	7.19	1.29	0.923
	Hg ²⁺	8.06	1.53	0.891

The composition of ACAD-13

* was (AMPS (0.15 M), DAEMA (0.1 M), AC-chitosan (150 mg) and N-MBA (0.012 M)) and ACAD-0 (AMPS (0.15 M), DAEMA (0.1 M), AC-chitosan (0 mg) and N-MBA (0.012 M)) and ACAD-21 (AMPS (0.15 M), DAEMA (0.1 M), AC-chitosan (150 mg) and N-MBA (0 M)). KPS (0.009 M) were taken in all the experiments for a polymerization volume of 40 mL.

3.9. Diffusion mechanism

The dye/metal ions and water uptake kinetics of ACAD-13 can be more quantitatively understood by fitting the initial swelling data (up-to 60%) of ACAD-13 in the following power law (Dhanapal & Subramanian, 2014) equation:

$$\frac{M_t}{M_\infty} = kt^n \quad (9)$$

where M_t is the amount of the water/or dye/or metal ion adsorbed by swollen polymer at time t , M_∞ is the amount of the water/or dye/or metal ion adsorbed after infinite time, k is the swelling constant related to the structure of network and n is the diffusion exponent. The values of n and k were calculated from the slope and

intercept of the plot $\log(M_t/M_\infty)$ vs. $\log(t)$, respectively, at different temperatures. In case of adsorption/or release from swellable matrices, if $n = 0.45\text{--}0.5$ then transport is nearly Fickian, whereas for $0.5 < n < 1$ the diffusion is non-Fickian. In the present investigation the values of n were found to be in the range of 0.66–0.74 for dye, metal ions solutions and pure water. These values indicated that the diffusion of dye/metal ions and water from the swollen polymer followed non-Fickian (Dhanapal & Subramanian, 2014) mechanism.

3.10. Desorption and reusability of adsorbent

In order to find the predominant mechanism for metal ions uptake, the pure water was eluted through metal ions adsorbed

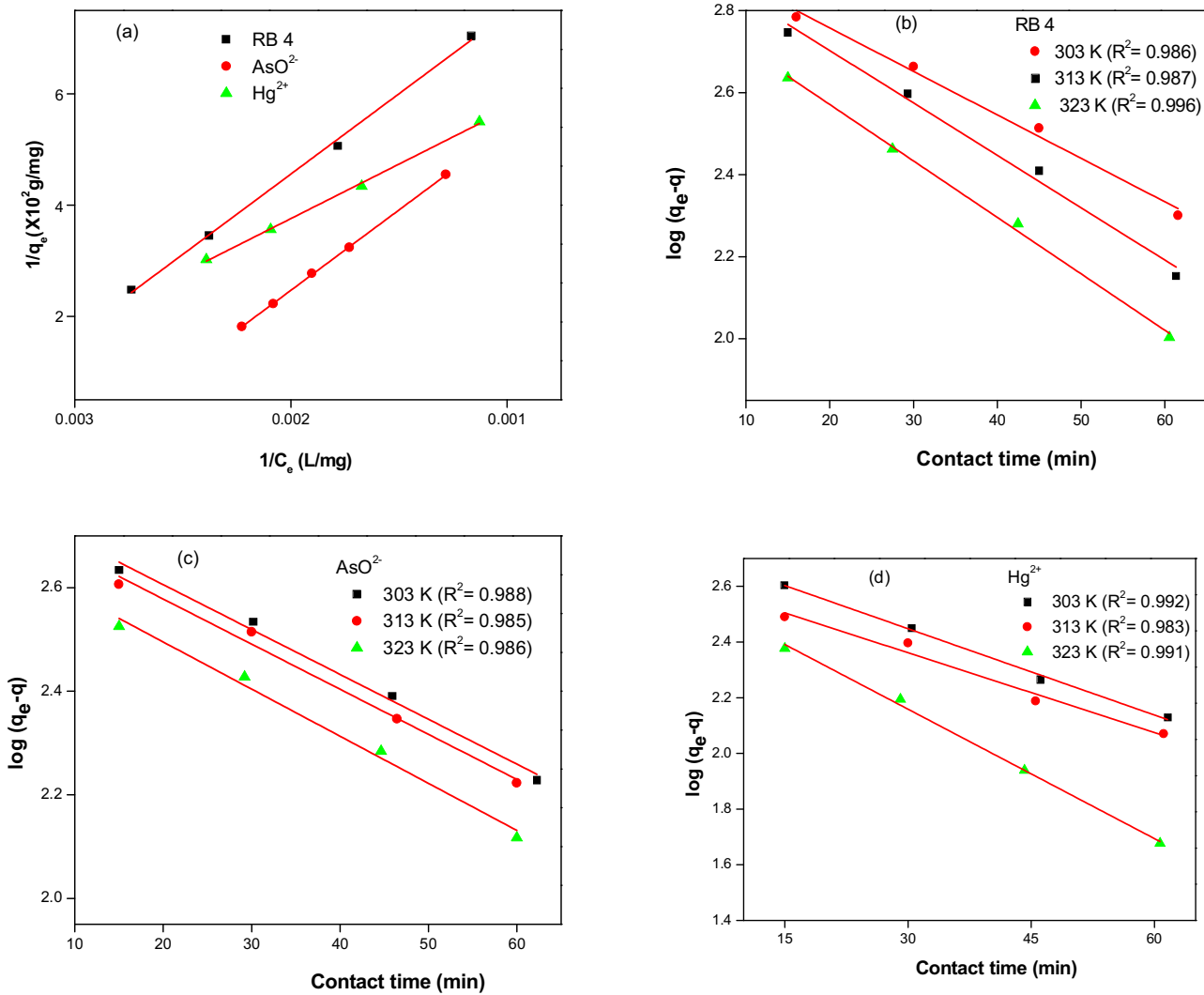


Fig. 4. Langmuir adsorption isotherms (a) and pseudo-first-order adsorption kinetic plots at different temperatures for ACAD-13/RB4 (b), ACAD-13/AsO²⁻ (c) and ACAD-13/Hg²⁺ (d) system.

Table 2

Pseudo-first and second order kinetics parameters for adsorption of ACAD-13/RB4, ACAD-13/AsO²⁻ and ACAD-13/Hg²⁺ systems at different temperatures.

Adsorbent code	Adsorbate	Kinetic model	T (K)	parameters($q_e = \text{mg/g}$, $k_1 = \text{min}^{-1}$ and $k_2 = \text{g/mg/min}$)	R^2
ACAD-13	RB4	Pseudo-first order	303	$q_e = 689.2, k_1 = 4.2$	0.998
			313	$q_e = 304.4, k_1 = 1.7$	0.999
			323	$q_e = 282.5, k_1 = 1.3$	0.998
	AsO ²⁻		303	$q_e = 525.4, k_1 = 3.4$	0.988
			313	$q_e = 312.6, k_1 = 2.6$	0.985
			323	$q_e = 178.2, k_1 = 1.6$	0.986
	Hg ²⁺		303	$q_e = 385.5, k_1 = 3.2$	0.992
			313	$q_e = 311.3, k_1 = 2.6$	0.983
			323	$q_e = 141.3, k_1 = 1.6$	0.991
ACAD-13	RB4	Pseudo-second order	303	$q_e = 77.3, k_2 = 5.23$	0.977
			313	$q_e = 42.2, k_2 = 4.65$	0.974
			323	$q_e = 31.7, k_2 = 4.50$	0.987
	AsO ²⁻		303	$q_e = 51.5, k_2 = 4.67$	0.852
			313	$q_e = 21.4, k_2 = 3.25$	0.911
			323	$q_e = 18.9, k_2 = 2.45$	0.883
	Hg ²⁺		303	$q_e = 45.8, k_2 = 3.45$	0.889
			313	$q_e = 20.4, k_2 = 2.34$	0.747
			323	$q_e = 18.9, k_2 = 2.10$	0.778

ACAD-13 and metal ions adsorbed/chelated virgin chitosan packed columns under identical conditions over a known and constant period of time. The amount of metal ions leached from ACAD-13 and virgin chitosan were found to be 189, 31 and 156 (mg/g), and

16 mg/g of AsO²⁻ and Hg²⁺, respectively. The differences were more likely attributed to the more metal ions uptake in three dimensional network ACAD-13 and the reduction in the concentration of free amino group available for metal chelation compared to

Table 3Thermodynamic parameters for adsorption of ACAD-13/RB4, ACAD-13/AsO²⁻ and ACAD-13/Hg²⁺ systems at different temperatures.

Adsorbent code	Adsorbate	T (K)	ΔG° (kJ/mol)	ΔH° (kJ/mol)	ΔS° (J/mol/K)	R^2
AsO ²⁻	AsO ²⁻	303	-21.1734	-47.43	15.45	0.987
		313	-6.53991			
		323	-4.59294			
Hg ²⁺	Hg ²⁺	303	-41.3379	-66.16	21.99	0.988
		313	-20.6205			
		323	-4.66825			
RB4	RB4	303	-21.4211	-48.44	15.12	0.997
		313	-9.72515			
		323	-3.76919			

virgin chitosan. Further, the reliability of adsorbent for the repeated usage in effluent treatment was tested by evaluating its reusability by several adsorption-desorption cycles using 0.01 M HCl as desorption agent. About 98% of metal ions and dye were recovered for more than five adsorption–desorption cycles. Hence ACAD-13 can be used repeatedly without losing its adsorption capacities for prolonged application.

3.11. Effect of AC-chitosan and N-MBA concentration in the feed and pH on uptake

Analysis of dye, metal ions and water uptake characteristics of all ACAD samples revealed that the ACAD-13 had adsorbed maximum dye and metal ions under ambient conditions but ACAD-0 had adsorbed pure water to the extent of 1189 g/g. However the uptake of metal ions/dye and thermal stability of ACAD-0 were significantly reduced due to low crosslink density and the lack of coordination sites.

The influence of crosslinker concentration on water uptake profile is shown Fig. 2(c). The uptake behavior of ACAD was directly and inversely proportional to crosslinker concentrations for low and high concentrations of crosslinker, respectively. For the crosslinker concentration 0.012 M, water, dye, AsO²⁻ and Hg²⁺ ions uptake were enhanced to the maximum values of 1055 g/g and 701, 551 and 455 mg/g, respectively which were reduced to 532 g/g and 412, 307, 524 mg/g, respectively without crosslinker.

The pH of the effluent affects the adsorption behavior of an adsorbent and its effect was investigated over a pH range of 2–12 and the results are displayed in Fig. 2(d). The functional groups on the surface of adsorbent may be altered by the variation in pH of dye effluent. It was obvious that the adsorption/chelation capacity increased with increasing pH of dye/metal ions in effluents, and significant enhancement on adsorption was observed when the pH value reached 6.5 and further increase of pH beyond 8 had reduced the dye/metal ion uptake. In acidic pH most of the $-\text{SO}_3^-$ groups on the surface of the adsorbent exist as $-\text{SO}_3\text{H}$, which lead to a competition between hydrogen ion and RB4/or AsO²⁻/or Hg²⁺ to seek the active site on the adsorbent. In basic pH (>9) the electrostatic repulsive force between adsorbent and adsorbate may minimize the dye/metal ions uptake.

4. Conclusions

Chitosan was modified by graft copolymerization using hydrophilic water soluble acrylic monomers to enhance its adsorption/chelation capacity for the collection of RB4, toxic metal ions AsO²⁻ and Hg²⁺ from aqueous media. The observed adsorption/chelation capacity values of the modified chitosan were significantly higher (701, 551 and 455 mg/g, respectively) than those reported for chitosan and chitosan based other adsorbent materials. The degree of acryloylation determined by ¹H NMR in AC-chitosan was found to be 0.282. TG studies of ACAD revealed that they are thermally stable under ambient environmental

conditions. The surface morphology by SEM on ACAD confirmed the presence of pores and network structures. The equilibrium dye adsorption at different dye/metal ion concentrations implied predominantly Langmuir isotherm model with pseudo-first order kinetics. The diffusion of water, dye and toxic metal ions into the matrix followed non-Fickian mechanism. The values of ΔG° , ΔH° and ΔS° for RB4, AsO²⁻ and Hg²⁺ adsorption/chelation indicated that the adsorption was spontaneous and exothermic for the chosen ACAD-13. These features demonstrated that ACAD-13 can serve as a potential adsorbent for the effective removal of reactive dyes and toxic metal ions from the aqueous media.

Acknowledgments

The authors thank the management of Bannari Amman Institute of Technology, Sathyamangalam for encouraging research work by extending the required facilities and IIT Madras (SAIF) for providing NMR characterization facilities.

References

- Ajai, P., Sunita, G., & Gupta, V. K. (2000). A new system for the spectrophotometric determination of arsenic in environmental and biological samples. *Analytica Chimica Acta*, 408, 111–115.
- Anoop Krishnan, K., & Anirudhan, T. S. (2002). Removal of mercury(II) from aqueous solutions and chlor-alkali industry effluent by steam activated and sulphurised activated carbons prepared from bagasse pith: Kinetics and equilibrium studies. *Journal of Hazardous Materials*, 92, 161–183.
- Baskaralingam, P., Pulikesi, M., Ramamurthi, V., & Sivanesan, S. (2006). Equilibrium studies for the adsorption of acid dye onto modified hectorite. *Journal of Hazardous Materials*, 136, 989–992.
- Bayramoglu, G., Yakup Arica, M., & Bektas, S. (2007). Removal of Cd(II), Hg(II) and Pb(II) ions from aqueous solution using p(HEMA)/Chitosan) membranes. *Journal of Applied Polymer Science*, 106, 169–177.
- Crini, G., & Badot, P. M. (2008). Application of chitosan, a natural aminopolysaccharide, for dye removal from aqueous solutions by adsorption processes using batch studies: A review of recent literature. *Progress in Polymer Science*, 33, 399–447.
- Dhanapal, V., & Subramanian, K. (2014). Recycling of textile dye using double network polymer from sodium alginate and superabsorbent polymer. *Carbohydrate Polymers*, 108, 65–74.
- Dhanapal, V., Vijayakumar, V., & Subramanian, K. (2013). Synthesis and evaluation of trimethylolpropane triacrylate crosslinked superabsorbent polymers for conserving water and fertilizers. *Journal of Applied Polymer Science*, 129, 1350–1361.
- Dhopakar, R., Rao, N. N., Pande, S. P., & Kaul, S. N. (2006). Removal of basic dyes from aqueous medium using a novel polymer: Jalshakti. *Bioresource Technology*, 97, 877–885.
- Diao, H., Yan, F., Qiu, L., Lu, J., Lu, X., Lin, B., et al. (2010). High performance cross-linked poly(2-acrylamido-2-methylpropanesulfonic acid)-based proton exchange membranes for fuel cells. *Macromolecules*, 43, 6398–6405.
- Dinesh, M., & Pittman, C. U., Jr. (2007). Arsenic removal from water/wastewater using adsorbents—A critical review. *Journal of Hazardous Materials*, 142, 1–53.
- Guilherme, M. R., Reis, A. V., Takahashi, S. H., Rubira, A. F., Feitosa, J. P. A., & Muniz, E. C. (2005). Synthesis of a novel superabsorbent hydrogel by copolymerization of acrylamide and cashew gum modified with glycidyl methacrylate. *Carbohydrate Polymers*, 61, 464–471.
- Jayakumar, R., Prabaharan, M., Reis, R. L., & Mano, J. F. (2005). Graft copolymerized chitosan—present status and applications. *Carbohydrate Polymers*, 62, 142–158.
- Liu, B., Wang, D., Yu, G., & Meng, X. (2013). Adsorption of heavy metal ions, dyes and proteins by chitosan composites and derivatives—A review. *Journal of Ocean University of China*, 12, 500–508.

- Musico, Y. L. F., Santos, C. M., Dalida, M. L. P., & Rodrigues, D. F. (2013). Improved removal of lead(II) from water using a polymer-based graphene oxide nanocomposite. *Journal of Materials Chemistry A*, *1*, 3789–3796.
- Muzzarelli, R. A. A. (1977). *Chitin*. Oxford: Pergamon Press.
- Muzzarelli, R. A. A. (2011). Potential of chitin/chitosan-bearing materials for uranium recovery: An interdisciplinary review. *Carbohydrate Polymers*, *84*, 54–63.
- Muzzarelli, R. A. A., & Rocchetti, R. (1974). The use of chitosan columns for the removal of mercury from waters. *Journal of Chromatography*, *96*, 115–121.
- Nami Kartal, S., & Imamura, Y. (2005). Removal of copper, chromium, and arsenic from CCA-treated wood onto chitin and chitosan. *Bioresource Technology*, *96*, 389–392.
- Paulino, A. T., Guilherme, M. R., Reis, A. V., Campese, G. M., Muniz, E. C., & Nozaki, J. (2006). Removal of methylene blue dye from an aqueous media using superabsorbent hydrogel supported on modified polysaccharide. *Journal of Colloid and Interface Science*, *301*, 55–62.
- Pourjavadi, A., Jahromi, P. E., Seidi, F., & Salimi, H. (2010). Synthesis and swelling behavior of acrylated starch-g-poly(acrylic acid) and acrylated starch-g-poly(acrylamide) hydrogels. *Carbohydrate Polymers*, *79*, 933–940.
- Pourjavadi, A., & Barzegar, S. (2009). Synthesis and evaluation of pH and thermosensitive pectin-based superabsorbent hydrogel for oral drug delivery systems. *Starch-Starke*, *61*, 161–172.
- Rajeswari, S., Namasivayam, C., & Kadirvelu, K. (2001). Orange peel as an adsorbent in the removal of acide violet 17(acid dye) from aqueous solution. *Waste Management*, *21*, 105–110.
- Siva Bharathi, Y., Mohan Reddy, M., Ramachandra Reddy, G., & Venkata Naidu, S. (2010). Synthesis, characterization and compatibility studies of homopolymers of poly(carboxy phenyl acrylate) and poly(carboxy methyl phenyl acrylate). *Malaysian Polymer Journal*, *5*, 95–108.
- Tahir, S. S., & Rauf, N. (2006). Removal of a cationic dye from aqueous solutions by adsorption onto bentonite clay. *Chemosphere*, *63*, 1842–1848.
- Tastan, B. E., Ertugrul, S., & Donmez, G. (2010). Effective bioremoval of reactive dye and heavy metals by *Aspergillus versicolor*. *Bioresource Technology*, *101*, 870–876.
- Wan Ngah, W. S., Teong, L. C., & Hanafiah, M. A. K. M. (2011). Adsorption of dyes and heavy metal ions by chitosan composites: A review. *Carbohydrate Polymers*, *83*, 1446–1456.
- Wang, J. J., & Liu, F. (2013). Enhanced adsorption of heavy metal ions onto simultaneous interpenetrating polymer network hydrogels synthesized by UV irradiation. *Polymer Bulletin*, *70*, 1415–1430.
- Yow loo, A. Y., Lay, Y. P., Kutty, M. G., Timpe, O., Behrens, M., & Abd-hamid, S. B. (2012). Spectrophotometric determination of mercury with iodide and rhodamine B. *Sains Malaysiana*, *41*, 213–218.
- Zhu, H. Y., Fu, Y. Q., Jiang, R., Yao, J., Xiao, L., & Zeng, G. M. (2012). Novel magnetic chitosan/poly(vinyl alcohol) hydrogel beads: Preparation, characterization and application for adsorption of dye from aqueous solution. *Bioresource Technology*, *105*, 24–30.